Dielectric, mechanical and thermal properties of ZrO_2-TiO_2 materials obtained by microwave sintering at low temperature

René M. Guillén[1*], Rut Benavente[1], María D. Salvador[1], Felipe L. Peñaranda[2], Paloma Recio[3], Rodrigo Moreno[3], Amparo Borrell[1]

[1]Instituto de Tecnología de Materiales (ITM), Universitat Politècnica de València, Camino de Vera, s/n, 46022 Valencia, Spain

[2]Instituto de las Tecnologías de la Información y Comunicaciones (ITACA), Universitat Politècnica de València, Camino de Vera s/n, 46022, Valencia, Spain

[3]Instituto de Cerámica y Vidrio, CSIC, Kelsen 5 28049 Madrid, Spain

*Corresponding author: Instituto de Tecnología de Materiales (ITM), Universitat Politècnica de València, Camino de Vera s/n, 46022, Valencia, Spain. Tel.: +34645603843; Fax: +34963877629.

E-mail address: reguipi@upv.es (René M. Guillén)

Abstract

The sinterability of 3Y-TZP/TiO_2 materials using micrometre-sized ZrO_2 and nanometre-sized TiO_2 (16 wt%) by one-step fast microwave sintering at low temperature (1200-1300 ºC) was investigated. Firstly, in situ detailed analysis of the dielectric properties of the material with temperature was carried out in order to measure the capacity of the material to transform microwave energy into heat. Another related parameter associated to microwave sintering is the penetration depth of the microwave radiation into the material, which showed great homogeneity from 400 ºC. Secondly, the effect of sintering conditions on microstructure, density, hardness and coefficient of thermal expansion was evaluated. The X-ray diffraction study and microstructural characterization demonstrate that it is possible to obtain fully dense pieces (>99%) by microwave sintering, a condition yielding to a coarse-grained (~1-2 μm), quite hard (~13.7 GPa) 3Y-TZP/TiO_2 material. However, the most important feature is the significant reduction of the thermal expansion coefficient ($8 \cdot 10^{-6}$ K^{-1}) as compared to that of 3Y-TZP. In addition, the results from conventional sintering at 1400-1500 ºC with 2 and 6 h of dwell time are examined and compared. The materials obtained at 1500 °C showed high density with grain size and hardness similar to those obtained by microwave but with a dramatic difference in the power consumption of the sintering cycle, since the materials obtained by microwave used a maximum absorbed power of 120 W and a heating cycle of only 40 min.

Keywords: ZrO_2-TiO_2; Microwave sintering; Sol-gel synthesis; Dielectric properties; Structural applications

1. Introduction

Ceramic materials are extensively employed in many technological areas present in our daily life. One of the most widely used ceramic materials is zirconium oxide (ZrO_2) or zirconia. However, at present the major drawback of zirconia materials as structural parts lies in their brittle behavior, which is associated with low reliability [1]. The addition of a second phase, such as TiO_2, allows considering novel applications in an expanding market, including reconstructive medicine (dentistry and orthopedics), the chemical and mineral processing industries as a grinding medium, and lightweight parts in structural applications [2]. In this context, zirconia-titania composites have also been used in the last decades as catalyst and support material in catalytic chemical reactions such as isomerization, hydrogenation and the selective reduction due to their noble metal interaction [3]. In addition, these zirconia-titania composites exhibit higher surface area [4,5]. Therefore, they have been regarded as an alternative support to bare TiO_2, to enhance sinterability over that of silica or alumina [6].

In a previous study, a research of the thermal expansion data of this material was done, demonstrating the great potential of zirconia-titania to be employed as a structural material and other applications that need high thermal performance and resistance [7]. There are various routes of synthesis for ZrO_2-TiO_2, one of the most widely studied being the sol-gel method [8]. After synthesis, these powders have to be sintered at high temperatures between 1300-1500 °C in conventional furnace during several hours holding time [9]. This is an important drawback due to the high added cost and longer production cycle time.

In a pioneering work, López-López et al. prepared dense $ZrTiO_4$ by slip casting of submicrometer sized Y-TZP and TiO_2 powders and subsequent reaction sintering [10,11]. The sintered materials exhibited a complex microstructure formed by $Zr_5Ti_7O_{24}$ as major phase and a secondary phase constituted by cubic zirconia in solid solution and a pyrochlore-type metastable phase ($Y_2Ti_{2-x}Zr_xO_7$) originated when using low soaking times. It was also demonstrated that the presence of zirconium titanate clearly reduced the thermal expansion coefficient of zirconia [12]. Spark plasma sintering has been also used for the preparation of zirconium titanate from submicron-sized zirconia and nanosized titania powders by reaction sintering at temperatures from 1300 ºC to 1400 ºC during 1 minute [13].

Therefore, to develop a new generation of advanced materials with exceptional properties that satisfy minimum requirements it is necessary not only to enhance the reactivity through a controlled synthesis but also to innovate in the process of sintering through simple and effective routes able to satisfy the demands for low cost and high energy efficiency. Therefore, the focus of this research is twofold: on one hand, to prepare powders by combining a simple colloidal sol-gel route and colloidal methods to guarantee a homogeneous dispersion of the components; on the other hand, to achieve full densification and high microstructural uniformity through a simple, fast sintering process while maintaining the properties and performance of the final materials. Microwave processing has appeared as a flexible form of energetics with many improvements over conventional heating, the most important

of which are: shorter time cycles, significant energy savings, and higher quality of the final material [14,15]. All these advantages, both energetic and economic, create a new vision for the future of ceramic materials and their industrial manufacturing.

The purpose of this work is to study the dielectric properties of the starting material composed of ZrO_2 and TiO_2, in order to understand the transformations that occur during the microwave sintering process. On this basis, the materials were sintered by microwave in one-step at temperatures of 1200 °C and 1300 °C and by conventional heating at 1400 °C and 1500 °C to compare the behavior of the materials produced by both sintering routes. Afterwards, an evaluation of the materials was performed by means of a study of the phases by X-ray diffraction and thermal expansion coefficient (TEC), aiming to analyze the internal changes of the material as a function of temperature. Finally, the materials were characterized in terms of density, hardness, and microstructure using Field Emission Scanning Electron Microscopy.

2. Materials and methods

2.1 Materials

Commercial submicrometer-sized ZrO_2 doped with 3 mol% Y_2O_3 (3Y-TZP, Tosoh TZ3YS, Tokyo, Japan) and a nanosized anatase-TiO_2 synthesized following the colloidal sol-gel route described elsewhere [16] were used as starting powders. The synthesis of TiO_2 was performed by dropwise addition of Ti (IV)-isopropoxide (97%, Sigma-Aldrich, Germany) on deionized water (18.2 $M\Omega \cdot cm^{-1}$, ultrapure Milli-Q) with a water:alkoxide molar ratio of 50:1. HNO_3 (65%, PANREAC, Spain) was utilized as a catalyst in a molar ratio of $H^+/Ti^{4+} = 0.2$. The synthesis was performed under constant stirring at a temperature of 50 °C in closed flask to prevent evaporation and maintained at these conditions for 24 h. At these conditions it was assured that peptization process was complete and the average particle size of the resulting suspension was 20-30 nm, as measured by dynamic light scattering (DLS, Zetasizer Nano ZS, Malvern S, Worcestershire, U.K). This nanoparticulate suspension was frozen using a rotary evaporator (RV10 basic, IKA, Germany) immersed in a liquid-N_2 bath, and subsequently freeze-dried (Cryodos-50, Telstar, Spain) at -50 °C and 0.3 mPa for 24 h.

Suspensions of the mixture were prepared to relative contents of 3Y-TZP/TiO_2 of 84/16 wt%. These materials react in a molar ratio 1:1 to produce $ZrTiO_4$, which means a weight ratio of about 60:40, but in this case the nanosized titania is intended to locally react wuth the coarser ZrO_2 particles to obtain reaction sintered $ZrTiO_4$ nanoparticles inside a zirconia matrix in order to modify some properties of the composite (in particular the coefficient of thermal expansion) while maintaining the excellent mechanical properties of zirconia. Suspensions were dispersed using an ammonium salt of poly(acrylic acid) (Duramax D-3005, Rohm & Haas, Dow Chemicals, USA) as a deflocculant in a concentration of 1.5 wt% (on a dry solids basis). The preparation of the suspension involved the addition of freeze dried TiO_2 nanopowder on deionized water containing the deflocculant in a first step, and the subsequent addition of 3Y-TZP powder maintaining mechanical stirring. Afterwards, the mixture was sonicated for 1 min using an external ice bath to prevent overheating. The solids content was maintained at 50 wt%. The final

suspension was frozen and subsequently freeze dried using the same equipment and conditions as for titania solutions. The final mixture of powders was sieved using a 37-µm mesh nylon sieve before sintering.

2.2 Measurement of dielectric properties of the powders and sintering processes

Microwave heating is conditioned by the dielectric properties of the material. These properties are defined by the following complex equation [17].

$$\varepsilon' = \varepsilon'_r - j \cdot \varepsilon''_r \qquad (1)$$

where ε'_r is the dielectric relative constant, expressing the ability of the material to store energy from an external source. The imaginary part (ε''_r) is the loss factor, that indicates the ability of the material to convert this energy into heat [18,19].

Another parameter related to microwave sintering is the penetration depth (D_p), described as the depth value at which power density falls to 1/e. This parameter allows estimating the optimal sample size to guarantee the volumetric heating in its entirety [20,21],

$$D_p = \frac{c}{2\pi f \sqrt{\frac{1}{2}\varepsilon'_r \left(\sqrt{1 + \left(\frac{\varepsilon''_r}{\varepsilon'_r}\right)^2} - 1 \right)}} \qquad (2)$$

where *c* is the vacuum speed of light and *f* is the frequency (close to 2.45 GHz).

The test was performed with samples of 10 mm in diameter and 15 mm in height, with a maximum peak incident power of 140 W and a final temperature of 1200 ºC. The specimens are placed in a quartz holder and introduced into the microwave cavity through an aperture. An IR pyrometer (OPTRIS GmbH, Germany) is used to measure the surface temperature of the quartz support from the side through an inspection hole in the cavity wall. A precise calibration process is applied to determine the volumetric temperature of the sample from surface temperature measurements.

For the sintering process, the obtained powders were compacted to obtain green materials with a cylindric shape. For this, a universal machine (Shidmazu AG-X Plus) with an applied pressure of 80 MPa was used to produce discs of 10 mm in diameter and 3 mm in height, which were then utilized for sintering experiments.

For conventional sintering (CS), the specimens were placed in an electric furnace (Carbolite GERO HTF 1800, Germany) at 1400 °C and 1500 °C in air with a heating ramp of 10 °C·min^{-1} and dwell times of 2 and 6 hours. Sintering temperatures were calibrated using PTCR FERRO rings, France.

For the microwave processing (MW), sintering was performed in an experimental oven consisting of a single-mode cylindrical cavity, at a resonance frequency of 2.45 GHz as heating cell. The parameters used were a temperature of 1200 °C and 1300 ºC in air with a heating rate of 50 °C·min^{-1} and 15 min dwell time at the maximal temperature. These parameters have been determined on the basis of previous studies of our research group in which it has been demonstrated that by means of these times and temperatures it is feasible to obtain materials with density near to the theoretical values [22,23].

2.3 Characterization of sintered materials

The crystalline phases of the sintered materials were determined by X-ray diffraction (XRD) with a D8 Advance diffractometer (Bruker, Germany) using Cu Kα radiation. The measurements were carried out in the interval 10º-80°, and the step size and the reading time were 0.02º and 0.2 s, respectively. The thermodiffractometric (TDX) studies were carried out on a Bruker D8 Advance Vantec diffractometer equipped in vacuum with an HTK 2000 variable temperature chamber (Germany). Patterns were obtained using Cu Kα radiation. The measurements were made in the 10º-70º range and the step size and time of reading were 0.02º and 0.2 s, respectively, at measurement intervals of 50 °C. The temperature ranged from room temperature to 1200 °C, with a heating rate of 10 °C·min^{-1}.

The relative density of the sintered material was determined by Archimedes' principle by submerging the sample in water (ASTM C373-14) [24]. Three different samples from each sintering condition were used for this analysis.

The microstructures of the specimens were analyzed by field emission scanning electron microscopy (FESEM, S4800 Hitachi, Japan). The thermal etching was performed for 30 min at 100 °C below the maximum temperature to reveal the grain boundaries. The average grain size of at least 500 grains was measured from the FESEM images using Image software according to the linear intercept method [25]. Images of two different samples from each sintering condition were analyzed.

Hardness (H) was analyzed with a nanoindenter equipment (G-200; Agilent Technologies, Spain) with a Berkovich tip for use on polished surfaces up to 1-µm using diamond paste. The tests were performed under a 1500 nm maximum depth control. Each specimen was tested with a 25-slit matrix, the amplitude of which was fixed at 2 nm at a frequency of 45 Hz. The average hardness values are established for the 400-1000 nm penetration depth range. Three different samples from each sintering condition were used for this analysis.

The thermal behavior of the sintered materials was analyzed by means of the thermal expansion coefficient (TEC) using a Netzsch DIL-402-C dilatometer with a sample holder and a fused silica probe. The temperatures studied ranged between 20 and 800 °C with a heating rate of 10 °C·min^{-1}. The sample dimensions were 12x10x3 mm.

Measurements were performed in triplicate on two different samples from each sintering condition and the TEC was averaged over the entire temperature range.

3. Results and Discussion

3.1 Dielectric properties of the material and sintering parameters

An exhaustive control of the microwave sintering was carried out during all cycle of heating, dwell time and cooling. Throughout the heating stage, the amount of energy supplied by the equipment was controlled to avoid overheating of the samples. During the cooling stage, the power supplied to the equipment was turned off and the samples were cooled freely, without microwave radiation. Figure 1 shows the profile of the power absorbed by the microwave and the temperature evolution during heating stage. The maximum power absorbed by the sample during the cycle is reached at maximum temperature and was only 120 W. The duration of the heating is slightly over 40 min. Considering that the dwell time is 15 min, the reduction of processing time between conventional and non-conventional methods is quite remarkable.

In general terms, energy absorption increases with temperature, except for some peaks at specific temperatures that could be assigned to the different stages of the sintering process. One of these peaks appears around 400 ºC, coinciding with an abrupt increase in temperature. To understand this gap, we focus on Figure 2, where the values of the dielectric constant and the loss factor as a function of temperature are shown.

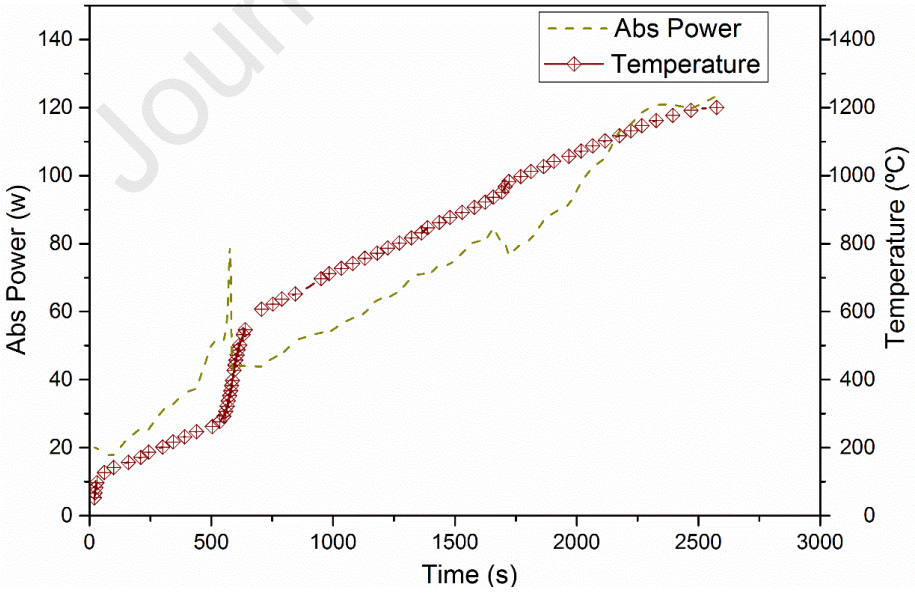

Figure 1. Microwave absorbed power and temperature profile during the sintering cycle.

The increase of the dielectric constant shows the capacity of the material to absorb microwave energy. At around 400 °C the energy absorbed by the material begins to be released as heat, therefore the loss factor starts to increase. Above that temperature, the dielectric constant remains uniform.

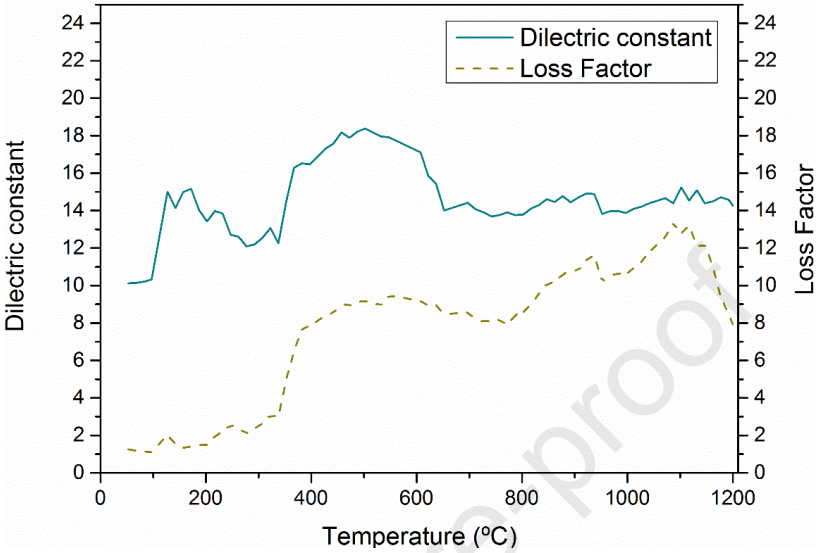

Figure 2. Dielectric constant and loss factor vs temperature of microwave sintered sample at 1200 ºC.

Figure 3 shows the evolution of the penetration depth of the microwave radiation as a function of temperature. The values of the penetration depth were calculated using equation (2). As the sample size is 15 mm in height and 10 mm in diameter, it should be noted that the depth of penetration guarantees a uniform distribution of the external electric field into the sample, preventing large temperature gradients.

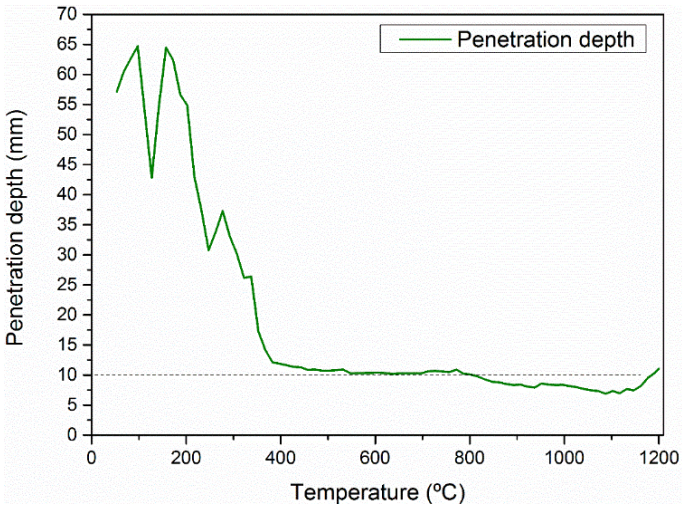

Figure 3. Penetration depth of microwave radiation at 2.45 GHz vs temperature for 3Y-TZP/TiO_2 sample.

3.2 Characterization of sintered materials

Density and grain size values for all samples obtained by conventional (CS) and microwave sintering (MW) are reported in Table 1. The theoretical density of the starting powder was measured with a helium pycnometer (AccuPyc 1330, Micromeritics, USA). The theoretical density of the material resulted to be ρ_{teor}: 5.12 g·cm^{-3}.

Table 1. Sintering conditions, relative density and average grain size values of 3Y-TZP/TiO_2 materials sintered by conventional (CS) and microwave technology (MW).

Sintering Method	Temperature (ºC)	Dwell time (min)	Relative density (%)	Grain size (µm)
CS	1400	120	95.7 ± 0.5	0.61 ± 0.01
	1400	360	96.2 ± 0.5	0.90 ± 0.01
	1500	120	98.0 ± 0.5	2.28 ± 0.02
	1500	360	98.9 ± 0.5	2.67 ± 0.02
MW	1200	15	99.3 ± 0.5	1.34 ± 0.02
	1300	15	99.5 ± 0.5	1.99 ± 0.02

The density values of the material treated at different temperatures in each sintering process clearly demonstrate that microwave technology leads to higher densification levels. An important observation is the lower density values obtained by conventional heating with respect to the non-conventional process, despite the higher temperatures and the longer dwell times employed. It is well observed that for CS at 1400 °C at 120 and 360 minutes of holding time density values of 95.7% and 96.2% are reached, with grain size values of 0.61 µm and 0.90 µm, respectively. Increasing the temperature to 1500 °C leads to an improvement in the density values but the grain size becomes more than twice that at 1400 ºC. Grain growth is a detrimental factor for materials whose structural applications are sensitive to the effects of temperature and thermal shocks, as the probability of failure due to thermal fatigue increases significantly.

On the other hand, highlighting the data obtained by microwave, there is a significant change in the values of both density and grain size with respect to those obtained by conventional sintering. The density values increase by approximately 3% up to near-to-theoretical values, while holding times are much lower. Consequently, grain size values are lower than expected for CS at the sintering temperatures necessary to get the same density.

Figure 4a shows the evolution of the diffraction patterns of 3Y-TZP/TiO_2 powders with temperature, measured in the range 30 ºC-1200 °C. Reflections at 2θ ~ 28º and 31º show the presence of a very small m-ZrO_2 content in the starting powder, indicating that the matrix is mainly formed by t-ZrO_2. The small crystalline size of TiO_2 (below 20

nm) does not allow detection of this phase. At the temperature transition between 400 and 600 °C, the diffusion of TiO_2 into ZrO_2 begins and the m-ZrO_2 disappears. The peaks corresponding to the crystalline zirconia phases t-ZrO_2 and c-ZrO_2 are identified with slight deviations from the pure patterns. This change in crystalline phases can be correlated to the dielectric properties around 400-600 ºC when the energy absorbed by the material is converted into heat. This change in the dielectric constant can occur when the diffusion of TiO_2 into the 3Y-TZP structure starts and ends at 600 ºC. This means that most of the titania is in solid solution in the zirconia lattice [26,27]. Above this temperature, the dielectric constant remains uniform and no further changes in the crystal structure are observed, as can be seen in the diffractogram at 1200 ºC.

Figure 4b shows the XRD diffractograms of 3Y-TZP/TiO_2 ceramic materials sintered by conventional (CS) and microwave sintering (MW) at different temperatures and dwell times. In all cases the same characteristic peaks of m-ZrO_2, t-ZrO_2 and c-ZrO_2 are observed. The tetragonal form of zirconia is the major phase in both materials but the content of the monoclinic phase in Ti doped- 3Y-TZP (CS) at 1500 ºC is higher than in the material sintered by MW at 1200 ºC. Rietveld refinements were performed using the structural models ICSD database: ICSD_86613.cif for $(Zr_{0.92}Y_{0.04}Ti_{0.04})$ O_2 tetragonal zirconia, ICSD_248792.cif for $Zr_{0.90}Y_{0.10}$ O_2 cubic zirconia, ICSD_41572.cif for ZrO_2 monoclinic zirconia and ICSD_79522.cif for $Y_2(Zr_{0.452}Ti_{0.55})_2O_7$ pyrochlore phase. By applying Fullprof program, the lattice parameters were indexed for t-ZrO_2 (P42 /nmc; $a = b$ = 3.5767 A, c = 5.1944 A, α = β= γ = 90º, tetragonality ratio c/a_f = 1.0269) and c-ZrO_2 (Fm-3m; a = 5.1148 A). They are in accordance with data reported by Lin in the system TiO_2-Y_2O_3-ZrO_2 [24]. The substitution of smaller Ti^{4+} ions (ionic radius = 0.074 nm) by Zr^{4+} (ionic radius = 0.084 n) and Y^{3+} (ionic radius = 0.1015 nm) ions in the tetragonal lattice, determines that the tetragonal lattice constant a_t decreases, while c_t and the tetragonality ratio (c_t/a_f) increases with respect to the tetragonal Y-TZP. XRD parameters in the 70º-80º 2θ region show the splitting of (400) and (004) reflections of tetragonal phase, while only the (400) line of cubic phase is present (Figure 5a). The XRD diffractogram at 2θ angles of 25º-35º (Figure 5b) shows a shoulder on the 2θ lower angle side of the (111) peak of the tetragonal phase, which suggests that a small amount of the pyrochlore phase, $Y_2(Zr,Ti)O_7$, may have formed, in good agreement with previous works [11,28].

In the case of conventional sintering, it is necessary to raise the temperature up to 1500 ºC to obtain densities of 98 %. Using microwave technology, it is possible to obtain dense 3Y-TZP/TiO_2 materials at much lower temperature (1200 °C) almost without m-ZrO_2, that means 300 ºC below maintaining densities above 99%. These results are in agreement with those also obtained conventionally by other authors [29,30].

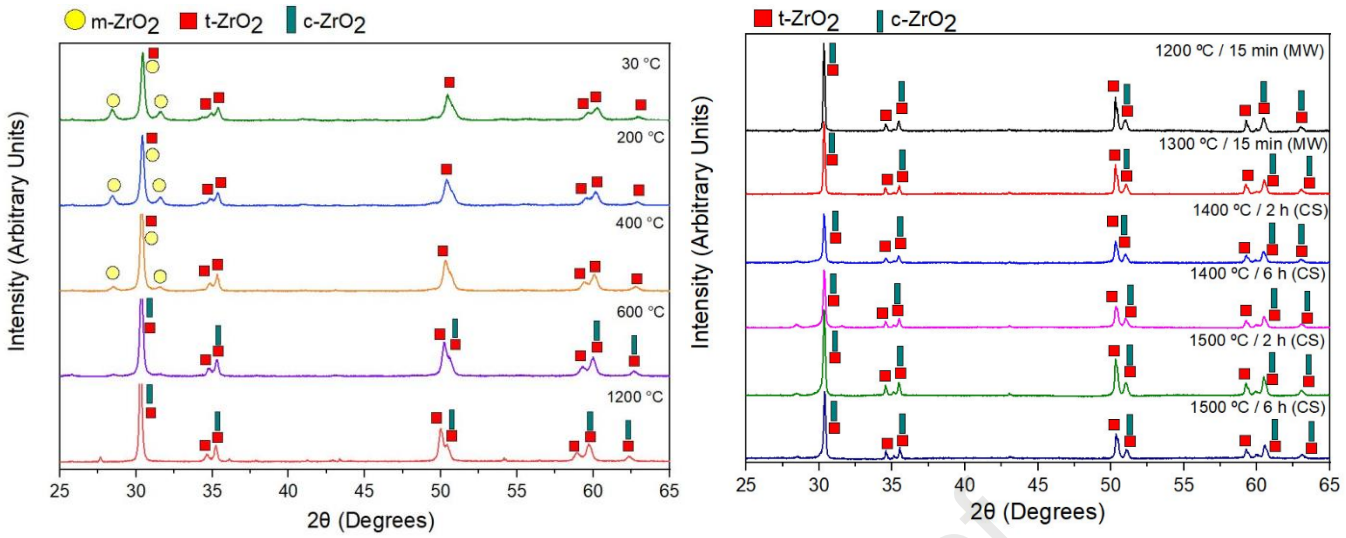

Figure 4. a) Evolution of the XRD patterns of 3Y-TZP/TiO_2 powders with temperature and, b) XRD patterns of 3Y-TZP/TiO_2 materials sintered by CS and MW at different temperatures and dwell times.

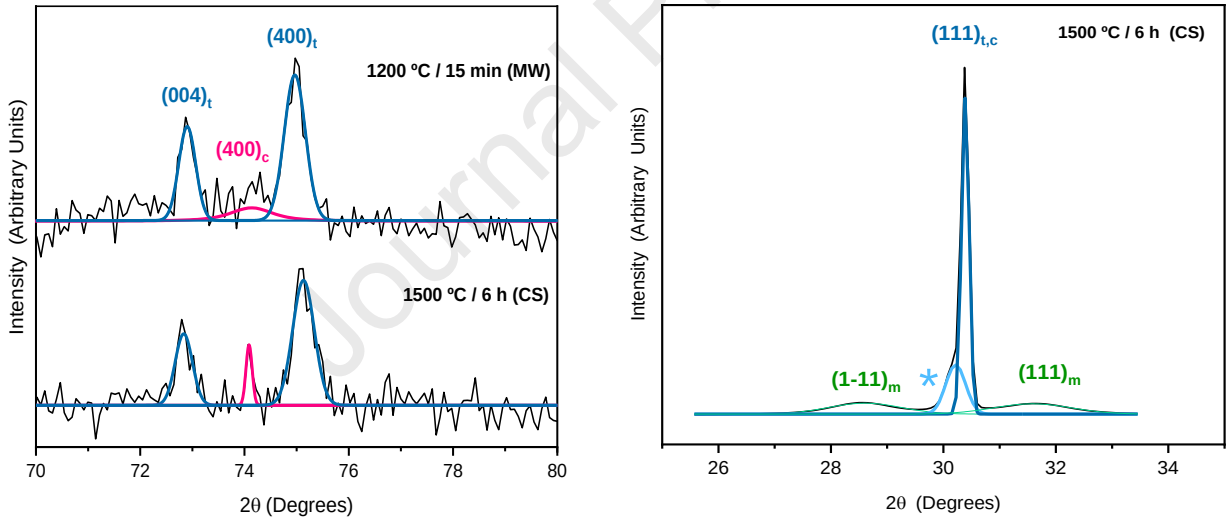

Figure 5. Deconvolution of the X-ray diffraction curves for 3Y-TZP/TiO_2 materials sintered by conventional (CS) and microwave technology (MW). The X-ray diffraction pattern, the fitting to the experimental curve and the peaks deconvolution are drawn; a) region 70º-80º 2θ, reflections (400) and (004) of tetragonal phase and line (400) of cubic phase. b) region 25º-35º 2θ, overlapping reflections (111) tetragonal and cubic phases, and peaks (1-11) and (111) of monoclinic phase. The shoulder at about 29.5º-30.5º 2θ of the diffraction profile suggests the existence of $Y_2(Zr,Ti)_2O_7$ pyrochlore.

3.3 Microstructure and properties

Figure 6 and Figure 7 show the differences in the microstructure of the materials sintered by both routes. The most important issue is the complete elimination of residual porosity in all the samples, which exhibit uniform microstructures with equiaxial grains. In spite of the much lower sintering temperature and dwell time the microstructure of the materials obtained by MW have smaller grain size than those obtained by CS. For CS materials it is possible to see that at 1500 ºC the increased dwell time from 2 to 6 h, only leads to a grain growth of ~15%, and the same occurs at 1400 ºC. As can be expected, the increase in sintering temperature led to an increase in grain size.

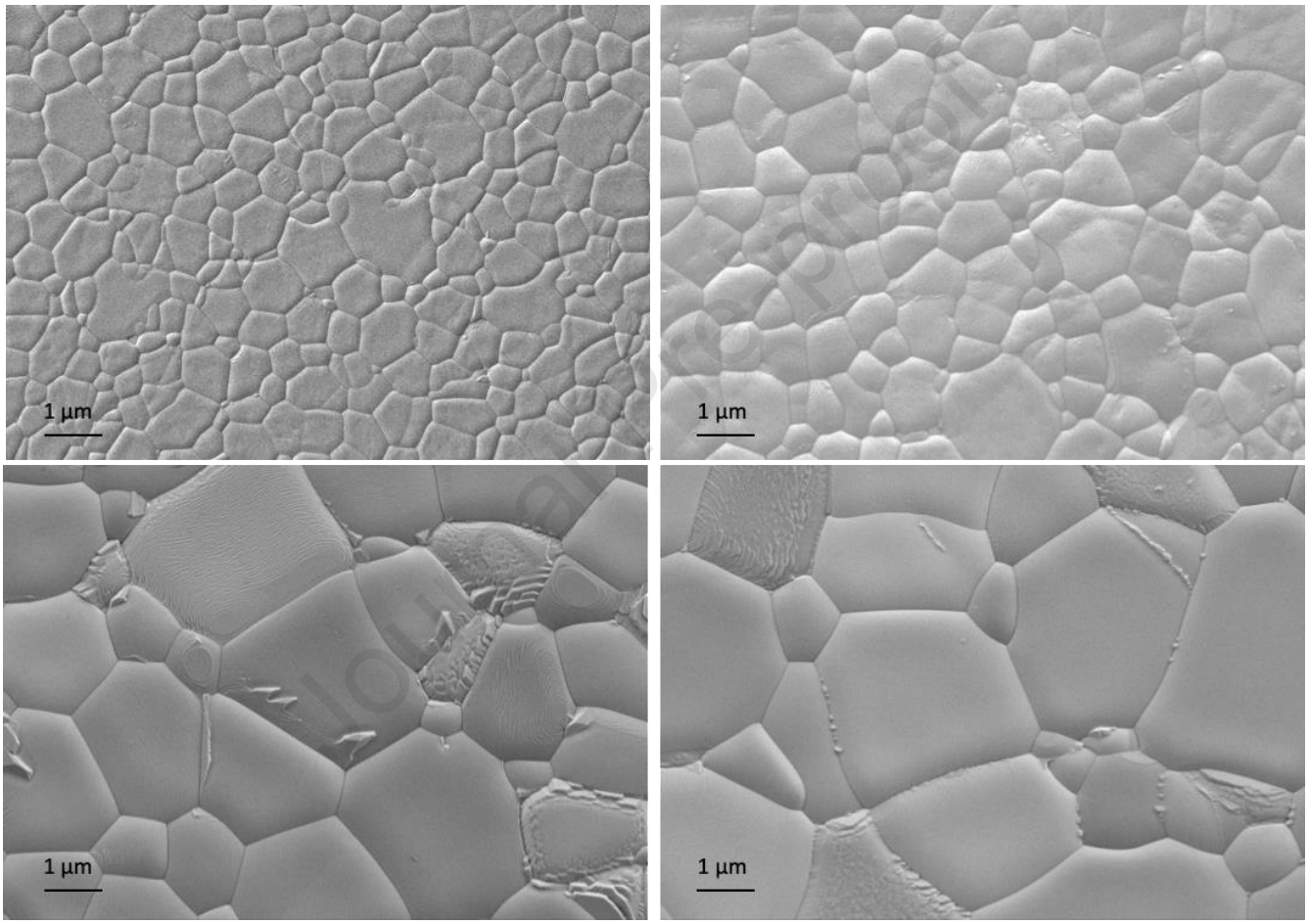

Figure 6. FE-SEM microstructures of 3Y-TZP/TiO_2 sintered by conventional sintering: a) 1400 ºC/2h, b) 1400 ºC/6h, c) 1500 ºC/2h and d) 1500 ºC/6h.

Using MW technology, it has been possible to obtain materials at very low temperatures and with densities ~99%. Considering the significant reduction in both the final temperature and the heating schedule, MW demonstrates to be an environmentally friendly and economically cost-effective process for massive production in the future.

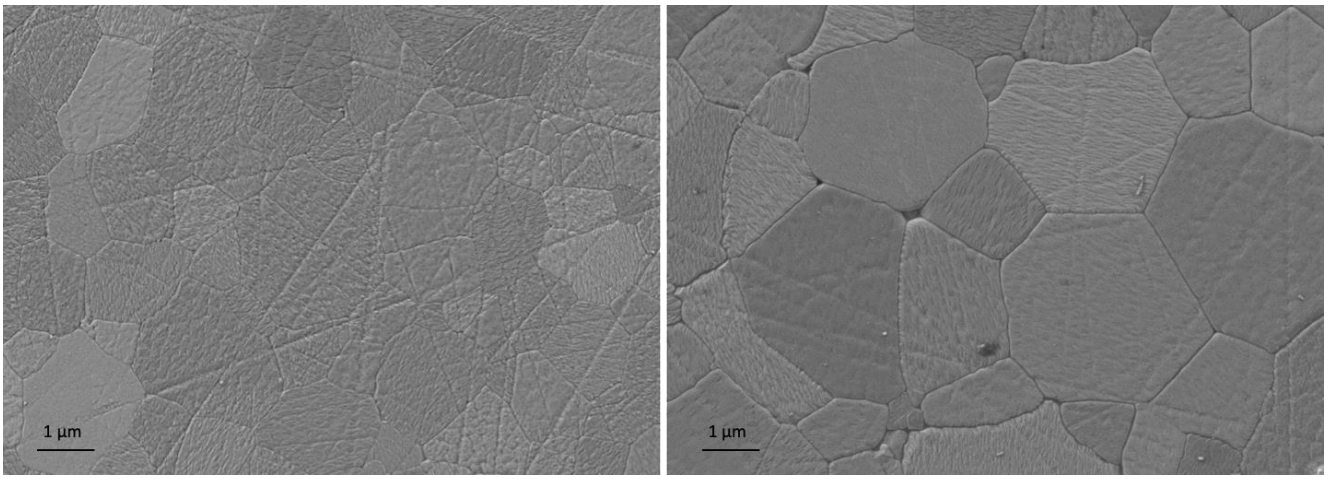

Figure 7. FE-SEM microstructures of 3Y-TZP/TiO_2 materials obtained by MW: a) 1200 ºC/15 min and b) 1300 ºC/15 min.

In Figure 8, the hardness (H) evolution with penetration depth is plotted. The large scatter of H for the initial 200 nm penetration depth could be due to the experimental variability implied by factors such as tip-sample interactions, roughness of the sample and tip rounding.

The average hardness values for the 400-1000 nm penetration depth range are as follows: CS-1400 ºC/2h 14.2 GPa; CS-1400 ºC/6h 12.8 GPa; CS-1500 ºC/2h 12.7 GPa; CS-1500 ºC/6h 11.4 GPa; MW-1200 ºC/15 min 13.7 GPa and MW-1300 ºC/15 min 13.2 GPa.

The highest hardness values obtained, both by conventional and non-conventional methods, are achieved in the samples sintered at lower temperature: CS-1400 ºC/2h and MW-1200 ºC/15min. This indicates that the grain size influences the results even more than the densification of the materials. In conventional sintering, increasing the dwell time from 2 to 6 h reduces the hardness values by ~ 10%. A similar reduction (~ 11%) is produced by increasing the temperature by 100 ºC.

Comparing the values obtained for the materials processed by MW, it is clear that an increase of 100 ºC in the final sintering temperature does not improve densification since the materials are close to the theoretical density, however, there is an increase of more than 48% in the grain size. This indicates that dense, high-hardness 3Y-TZP/TiO_2 composites can be obtained at only 1200 ºC and 15 min. If these values are compared with those obtained in the literature for the monolithic material 3Y-TZP, it is observed that the doping of zirconia with titania allows obtaining materials with similar mechanical properties and even lower temperatures [29-31].

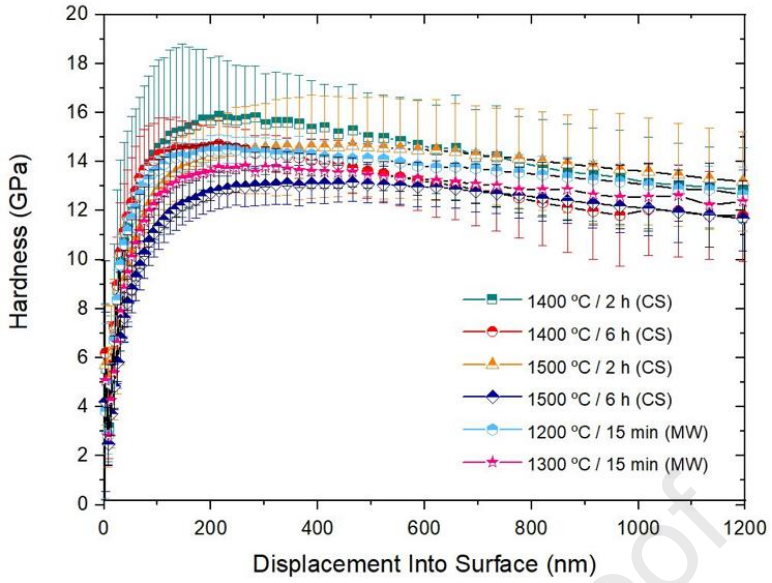

Figure 8. Hardness as a function of the test depth of the 3Y-TZP/TiO_2 sintered samples.

3.4 Thermal expansion coefficient (TEC)

Table 2 shows the average values of the coefficient of thermal expansion (or technical α values), for the sintered samples at different temperatures and processes, calculated in the temperature interval of 25-800 °C. In all cases, the trend of TEC values of sintered samples is the same: very controlled and close to $8 \cdot 10^{-6}$ K^{-1}. These data are in agreement with those found in the literature for 3Y-TZP/TiO_2 materials. These materials show great potential in structural applications involving thermal shock resistance requirements, since it exhibits crystallographic anisotropy in thermal expansion, with thermal expansion coefficient data between 8.1- 8.2 $\cdot 10^{-6}$ K^{-1} for temperature ranges from 25 ºC to 900 °C [32,33].

Grabowski et al., reported TEC data of $10.7 \cdot 10^{-6}$ K^{-1} measured in the same temperature ranges (25-800 ºC) for 3Y-TZP materials obtained by conventional sintering at 1500 ºC for 2 h. It should be noted the reduction of almost 30% of the TEC of the 3Y-TZP/TiO_2 composites with respect to 3Y-TZP, which results in a higher thermal stability in a wide temperature range [34].

The difference in TEC values for 3Y-TZP/TiO_2 are due to the processing used and the maximum sintering temperature. The values obtained for the microwave samples are slightly higher than those obtained by conventional sintering, although they cannot be compared each other, since the density values are significantly higher. It is observed that an increase of 100 ºC in the sintering temperature causes an increase in the TEC of 6% in CS and 8% in MW.

Table 2. Thermal expansion coefficient values of materials sintered by CS and MW.

Sintering Process	Temperature/Dwell time	TEC (10^{-6} K^{-1}) 25 to 800 °C

CS	1400 °C/2 h	7.52 ± 0.11
	1500 °C/2 h	8.01 ± 0.10
MW	1200 °C/15 min	7.61 ± 0.05
	1300 °C/15 min	8.26 ±0.14

These results demonstrate that microwave technology allows obtaining 3Y-TZP/TiO_2 materials with significantly higher thermal stability thanks to the reduction of the TEC value of 30%, while maintaining the same mechanical properties. Last, but not least, it is very remarkable the fact that this technology reduces the sintering temperature by 300 ºC with dwell times of only 15 min, which means a great energy saving with respect to conventional sintering.

4. Conclusions

It was demonstrated that the sinterability of 3Y-TZP/TiO_2 materials is strongly enhanced by the use of microwave sintering from mixtures of micro-ZrO_2 and nano-TiO_2 and this technology allowing the total energy input to decrease by 80%. The following main conclusions can be drawn from the experimental results and analysis:

1. The values of the dielectric properties and loss factor of the 3Y-TZP/TiO_2 materials allow to identify that the supplied energy for sintering permits the sufficient generation of thermal energy to obtain high density values and optimum hardness levels for applications requiring working exposures at high temperatures with low thermal expansion coefficients.

2. Hardness of these 3Y-TZP/TiO_2 advanced ceramics increases gradually with increasing sintering temperature until they reach high densification with null porosity.

3. The values of the thermal expansion coefficient are in good agreement with those reported in the literature ($8 \cdot 10^{-6}$ K^{-1}). A negligible increase in the TEC of the MW samples with respect to the CS samples is registered, probably associated to their higher density. In all cases, the TEC presents controlled values in a wide temperature range.

ACKNOWLEDGEMENTS

The authors are grateful to the Generalitat Valenciana for the funding support for the Santiago Grisolía program (GRISOLIAP/2018/168) and to the Ministry of Science, Innovation and Universities (Spain) through the projects RTI2018-099033-B-C32 and C33 (MCIU/AEI/FEDER, UE) and RYC-2016-20915.

REFERENCES

[1] J. R. Kelly, I. Denry. Stabilized zirconia as a structural material: an overview. Dent Mater, 24(3), 289-98, 2008.

[2] B. Basu, K. Balani, Advanced structural ceramics. Hoboken:Wiley; 2011.

[3] E. Setiawati and K. Kawano, "Stabilization of anatase phase in the rare earth; Eu and Sm ion doped nanoparticle TiO_2," *J. Alloys Compd.*, vol. 451, 1–2, 293-296, 2008.

[4] X. Yan *et al.*, "TiO_2 Nanomaterials as Anode Materials for Lithium-Ion Rechargeable Batteries," *Energy Technol.*, vol. 3, 8, 801-814, 2015.

[5] A. D. Modestov and O. Lev, "Photocatalytic oxidation of 2,4-dichlorophenoxyacetic acid with titania photocatalyst. Comparison of supported and suspended TiO_2," *J. Photochem. Photobiol. A Chem.*, vol. 112, 2-3, 261-270, 1998.

[6] X. Chen and S. S. Mao, "Titanium dioxide nanomaterials: Synthesis, properties, modifications and applications," *Chem. Rev.*, vol. 107, 7, 2891-2959, 2007.

[7] A. Borrell and M. D. Salvador, "Advanced ceramic materials: processes and applications," in *Advanced ceramic materials: processes and applications*, UPV, 2018, pp. 6-9.

[8] M. Vicent, E. Sanchez, I. Santacruz, and R. Moreno, "Dispersion of TiO_2 nanopowders to obtain homogeneous nanostructured granules by spray-drying," *J. Eur. Ceram. Soc.* 31, 1413-1419, 2011.

[9] T. A. Schaedler, W. Francillon, A. S. Gandhi, C. P. Grey, S. Sampath, and C. G. Levi, "Phase evolution in the $YO_{1.5}$-TiO_2-ZrO_2 system around the pyrochlore region," *Acta Mater.*, 53, 10, 2957-2968, 2005.

[10] E. López-López, C. Baudín, R. Moreno, Synthesis of zirconium titanate-based materials by colloidal filtration and reaction sintering, Int. J. Appl. Ceram. Technol., 5 [4] ,394-400, 2008.

[11] E. López-López, M. L. Sanjuán, R. Moreno, C. Baudín, Phase evolution in reaction sintered zirconium titanate based materials. *J Eur Ceram Soc*; 30:981-91, 2010.

[12] E. López-López, C. Baudín, R. Moreno, Thermal expansion of zirconia-zirconium titanate materials obtained by slip casting of mixtures of Y-TZP-TiO_2. *J Eur Ceram Soc*; 29:3219–25, 2009.

[13] A. Borrell, M. D. Salvador, V. G. Rocha, A. Fernández, A. Gómez, E. López-López, R. Moreno, $ZrTiO_4$ materials obtained by spark plasma reaction-sintering, Composites: Part B 56, 330–335, 2014.

[14] A. Borrell, M. D. Salvador, F. L. Peñaranda-Foix, and J. M. Cátala-Civera, "Microwave sintering of zirconia materials: mechanical and microstructural properties," *Int. J. Appl. Ceram. Technol.*, vol. 10, 2, 313–320, 2013.

[15] A. Borrell, F. L. Penaranda-Foix, M. D. Salvador, J. M. Catala-Civera, and M. Miranda, "Microwave technique: a powerful tool for sintering ceramic materials," *Curr. Nanosci.*, vol. 10, 1, 32–35, 2014.

[16] M. Borlaf, M. T. Colomer, F. Cabello, R. Serna, R. Moreno, Electrophoretic Deposition of TiO_2/Er^{3+}

Nanoparticulate Sols, J. Phys. Chem. B 2013, 117, 1556−1562.

[17] B. Garcia-Baños, J. M. Catalá-Civera, F. L. Peñaranda-Foix, P. Plaza-González, and G. Llorens-Vallés, "In situ monitoring of microwave processing of materials at high temperatures through dielectric properties measurement," *Materials (Basel).*, vol. 9, 5, 2016.

[18] C. Delerue and M. Lannoo, "Dielectric Properties." 77–103, 2004.

[19] R. Benavente, A. Borrell, M. D. Salvador, O. García-Moreno, F. L. Peñaranda-Foix, and Y. J. M. Catalá-Civera, "Propiedades mecánicas y coeficiente de dilatación térmica de la β-eucriptita sinterizada por la técnica de microondas," *Bol. Soc. Esp. Ceram. y Vidr.*, vol. 53, 3, 133–138, 2014.

[20] R. R. Mishra,A. K. Sharma, "Microwave-material interaction phenomena: Heating mechanisms, challenges and opportunities in material processing," *Compos. Part A Appl. Sci. Manuf.*, vol. 81, 78–97, 2016.

[21] R. Freer, F. Azough, "Microstructural engineering of microwave dielectric ceramics," *J. Eur. Ceram. Soc.*, vol. 28, 7, 1433–1441, 2008.

[22] A. Borrell, M, D. Salvador (October 31st 2018). Advanced Ceramic Materials Sintered by Microwave Technology, Sintering Technology - Method and Application, Malin Liu, IntechOpen, DOI: 10.5772/intechopen.78831.

[23] R. Benavente, A. Borrell, M. D. Salvador, O. Garcia-Moreno, F. L. Peñaranda-Foix, and J. M. Catala-Civera, "Fabrication of near-zero thermal expansion of fully dense β-eucryptite ceramics by microwave sintering," *Ceram. Int.*, vol. 40, 1, Part A, 935–941, 2014.

[24] ASTM C373-14, "Standard Test Method for Water Absorption, Bulk Density, Apparent Porosity, and Apparent Specific Gravity of Fired Whiteware Products," *Astm C373-88*, 1999.

[25] A. Standard, "ASTM E112-13: Standard test methods for determining average grain size," *Stand. Test Methods Determ. Aver. Grain Size." ASTM Int. West Conshohocken, PA*, 2013.

[26] R. B. Miranda, T. P. Leite, A. C. Fagundes, M. Martins, N. Batista, J. Marchi, P. F. Cesar, "Effect of titania addition and sintering temperature on the microstructure, optical, mechanical and biological properties of the Y-TZP/TiO2 composite" dental materials 36, 1418–1429, 2020.

[27] K. Thamaphat, P. Limsuwan, and B. Ngotawornchai, "Phase characterization of TiO2 powder by XRD and TEM," *Kasetsart J.(Nat. Sci.)*, vol. 42, 5, 357-361, 2008.

[28] C. L. Lin, D. Gan, P. Shen, "The effects of TiO_2 addition on the microstructure and transformation of ZrO_2 with 3 and 6 mol.% Y_2O_3," *Mater. Sci. Eng. A*, *129*(1), 147-155, 1990.

[29] A. Borrell, M. D. Salvador, F. L. Peñaranda-Foix, and J. M. Cátala-Civera, "Microwave sintering of Zirconia materials: Mechanical and microstructural properties," *Int. J. Appl. Ceram. Technol.*, vol. 10, 2, 313–320, 2013.

[30] A. Goldstein, N. Travitzky, A. Singurindy, and M. Kravchik, "Direct microwave sintering of yttria-stabilized zirconia at 2·45 GHz," *J. Eur. Ceram. Soc.*, vol. 19, 12, 2067-2072, 1999.

[31] D. D. Upadhyaya, A. Ghosh, G. K. Dey, R. Prasad, and A. K. Suri, "Microwave Sintering of Zirconia Ceramics," J. Mater. Sci., vol. 36, 19, 4707-4710, 2001.

[32] C. N. Chu, N. Saka, and N. P. Suh, "Negative thermal expansion ceramics: A review," *Mater. Sci. Eng.*, vol. 95, C, 303-308, 1987.

[33] I. Jin Kim and G. Cao, "Low thermal expansion behavior and thermal durability," *J. Eur. Ceram. Soc.*, vol. 22, 14-15, 2627-2632, 2002.

[34] G. Grabowski, R. Lach, Z. Pędzich, K. Świerczek, A. Wojteczko, "Anisotropy of thermal expansion of 3Y-TZP, a-Al2O3 and composites from 3Y-TZP/a-Al2O3 system" Arch Civ Mech Eng. 18 (2018) 188-197.

Table 1. Sintering conditions, relative density, and average grain size values of 3Y-TZP/TiO_2 materials sintered by conventional (CS) and microwave technology (MW).

Sintering Method	**Temperature (ºC)**	**Dwell time (min)**	**Relative density (%)**	**Grain size (µm)**
CS	1400	120	95.7 ± 0.5	0.61 ± 0.01
	1400	360	96.2 ± 0.5	0.90 ± 0.01
	1500	120	98.0 ± 0.5	2.28 ± 0.02
	1500	360	98.9 ± 0.5	2.67 ± 0.02
MW	1200	15	99.3 ± 0.5	1.34 ± 0.02
	1300	15	99.5 ± 0.5	1.99 ± 0.02

Table 2. Thermal expansion coefficient values of materials sintered by CS and MW.

Sintering Process	Temperature/Dwell time	TEC (10^{-6} K^{-1}) 25 to 800 °C
CS	1400 °C/2 h	7.52 ± 0.11
	1500 °C/2 h	8.01 ± 0.10
MW	1200 °C/15 min	7.61 ± 0.05
	1300 °C/15 min	8.26 ±0.14